



LAWRENCE  
LIVERMORE  
NATIONAL  
LABORATORY

# Impact of particle shape on the laser-contaminant interaction induced damage on the protective capping layer of 1w high reflector mirror coatings

S. R. Qiu, M. A. Norton, J. Honig, A. M. Rubenchik, C. D. Boley, A. Rigatti, C. J. Stolz, M. J. Matthews

December 15, 2015

SPIE Optical Engineering  
Boulder, CO, United States  
September 27, 2015 through September 30, 2015

## **Disclaimer**

---

This document was prepared as an account of work sponsored by an agency of the United States government. Neither the United States government nor Lawrence Livermore National Security, LLC, nor any of their employees makes any warranty, expressed or implied, or assumes any legal liability or responsibility for the accuracy, completeness, or usefulness of any information, apparatus, product, or process disclosed, or represents that its use would not infringe privately owned rights. Reference herein to any specific commercial product, process, or service by trade name, trademark, manufacturer, or otherwise does not necessarily constitute or imply its endorsement, recommendation, or favoring by the United States government or Lawrence Livermore National Security, LLC. The views and opinions of authors expressed herein do not necessarily state or reflect those of the United States government or Lawrence Livermore National Security, LLC, and shall not be used for advertising or product endorsement purposes.

# Impact of particle shape on the laser-contaminant interaction induced damage on the protective capping layer of $1\omega$ high reflector mirror coatings

S.R. Qiu<sup>1,\*</sup>, M.A. Norton<sup>1</sup>, J. Honig<sup>1</sup>, A.M. Rubenchik<sup>1</sup>, C.D. Boley<sup>1</sup>, A. Rigatti<sup>2</sup>, C.J. Stolz<sup>1</sup>, and M.J. Matthews<sup>1</sup>

<sup>1</sup>Lawrence Livermore National Laboratory, 7000 East Avenue, Livermore, CA 94551

<sup>2</sup>Laboratory for Laser Energetics, University of Rochester, 250 E. River Rd., Rochester NY 14623

\*Corresponding author: [giu2@llnl.gov](mailto:giu2@llnl.gov), Phone: (925) 422-1636 Fax: (925) 423-0792

## Abstract

We report an investigation on the response to laser exposure of a protective capping layer of  $1\omega$  (1053 nm) high-reflector mirror coatings, in the presence of differently shaped Ti particles. We consider two candidate capping layer materials, namely  $\text{SiO}_2$  and  $\text{Al}_2\text{O}_3$ . They are coated over multiple silica-hafnia multilayer coatings. Each sample is exposed to a single oblique ( $45^\circ$ ) shot of a 1053 nm laser beam (p polarization, fluence  $\sim 10 \text{ J/cm}^2$ , pulse length 14 ns), in the presence of spherically or irregularly shaped Ti particles on the surface. We observe that the two capping layers show markedly different responses. For spherically shaped particles, the  $\text{Al}_2\text{O}_3$  cap layer exhibits severe damage, with the capping layer becoming completely delaminated at the particle locations. In contrast, the  $\text{SiO}_2$  capping layer is only mildly modified by a shallow depression, likely due to plasma erosion. For irregularly shaped Ti filings, the  $\text{Al}_2\text{O}_3$  capping layer displays minimal to no damage while the  $\text{SiO}_2$  capping layer is significantly damaged. In the case of the spherical particles, we attribute the different response of the capping layer to the large difference in thermal expansion coefficient of the materials, with that of the  $\text{Al}_2\text{O}_3$  about 15 times greater than that of the  $\text{SiO}_2$  layer. For the irregularly shaped filings, we attribute the difference in damage response to the large difference in mechanical toughness between the two materials, with that of the  $\text{Al}_2\text{O}_3$  being about 10 times stronger than that of the  $\text{SiO}_2$ .

**Keyword:** Protective coating layer, High reflector, Multilayer coatings, Laser damage, Plasmas,  $1\omega$ , 1064 nm, High peak power laser.

## 1. Introduction

Surface contamination can lower laser damage resistance of high reflector mirrors made of dielectric multilayer coatings in high-peak-power laser systems, including the National Ignition Facility (NIF), Laser Megajoule, and OMEGA [1-3]. Handling and processing may contribute to contaminations, but the major contamination sources are components that surround the mirrors within the laser system [4-6], such as beam dumps and fasteners. Typical contaminants that have been found include both organic and inorganic materials, such as oil, polyester fibers, ceramics, metal/metal oxides, and alloys. In addition to having a large distribution of the chemical contents, contaminants also have a variety of morphologies including sphere, rectangular, or irregular shape.

For high reflective multilayer coatings, adding an absentee overcoat or protective capping layer above the outmost layer has been shown to increase the resistance to laser-induced damage [7-9]. A similar strategy of adding a protective capping layer has also been adopted to extend the lifetime of multilayer mirrors in extreme ultraviolet lithography applications [10]. However, the underlying mechanism by which the coupling between the laser and contaminant causes damage to the protective layer is still elusive. In order to facilitate effective selection and design of capping materials and to develop a practical solution for contaminant removal, an improved understanding of the physical principles is desirable.

An early study showed that the laser-induced damage to the reflective surface is strongly dependent on the contaminant composition and size, as well as the laser fluence [11]. In the present work, we extend that study to explore how the laser-induced damage depends on the contaminant shape. We use Ti particles, a common surface contaminant found on

NIF mirrors, having different shapes. One selected shape is spherical, and another shape is irregular (croissant like). To account for the role of the highly reflective surface, we utilize an oblique angle of incidence of the laser beam. Specifically, in the given geometry, we investigate the response of the capping layer under 45° oblique irradiation of a single pulse of laser light (1053 nm, p-polarized, fluence ~10 J/cm<sup>2</sup>, pulse length 14 ns), in the presence of both spherically- and irregularly-shaped Ti particles. The high reflector (>99.5% HR) samples were silica-hafnia multilayer coatings fabricated by e-beam physical vapor deposition (e-PVD). Silica-hafnia multilayers are commonly used for high reflectors in high peak-power laser systems which require high laser damage resistance [12, 13]. The capping layer materials are Al<sub>2</sub>O<sub>3</sub> and the previously used SiO<sub>2</sub> [8], respectively. Al<sub>2</sub>O<sub>3</sub> is a large bandgap material with a large thermal expansion coefficient and high mechanical strength. It has been shown to have high laser-damage resistance [14-16]. Recent studies have demonstrated that this material can be successfully integrated with silica-hafnia multilayer coatings by e-PVD for large-aperture high-fluence laser systems [13].

We find that under similar exposure conditions, the response of the capping layer to laser-particle interaction demonstrates a great contrast and is strongly dependent on the Ti particle shape. For aspherically-shaped Ti particle, the laser induced damage is more pronounced on the Al<sub>2</sub>O<sub>3</sub> capping surface than on the SiO<sub>2</sub> capping surface. The observed difference is attributed to heating of the substrate by the ablated plasma and the large disparity in the thermal expansion coefficients of the two capping materials, with that of Al<sub>2</sub>O<sub>3</sub> layer being about 15 times greater than that of SiO<sub>2</sub> [17]. On the other hand, for irregularly-shaped Ti particles, plasma mainly ablates outward, producing recoil momentum, and the laser-induced damage is more severe on the SiO<sub>2</sub> surface than on the Al<sub>2</sub>O<sub>3</sub> layer. This difference is related to the large difference in mechanical toughness between the two materials, with that of Al<sub>2</sub>O<sub>3</sub> much greater than that of the SiO<sub>2</sub>. Our findings provide fundamental criteria for the selection of high laser damage resistance materials for different applications.

## 2. Experimental Method

### 2.1 Coating Sample Preparation

The high reflector (>99.5% R) coatings were designed for a 1053 nm center wavelength, 45° angle of incidence, and p-polarization application. The design utilized 35 quarter-wave layers of alternating hafnia and silica with a half-wave top capping layer of either Al<sub>2</sub>O<sub>3</sub> (thickness: 360 nm) or SiO<sub>2</sub> (thickness: 410 nm). The multilayer high reflector samples with different capping layer compositions were fabricated through physical vapor deposition in a 54-in. or a 56-in. vacuum chamber equipped with quartz heater lamps, dual electron-beam guns, multi-point quartz crystal monitors, a planetary substrate rotation, and cryopumps. Granular SiO<sub>2</sub> was evaporated from a continuously rotating pan while Hf metal or Al<sub>2</sub>O<sub>3</sub> granules were deposited from a stationary six-pocket electron-beam gun [18]. The chamber was back-filled with oxygen during deposition of the Hf layers in order to oxidize the vapor plume at the substrate, resulting in a thin film coating of HfO<sub>2</sub>. The oxygen back-fill for the SiO<sub>2</sub> and Al<sub>2</sub>O<sub>3</sub> layers was optimized for thin film stress control while simultaneous not significantly impacting the deposited material stoichiometry [13, 19].

### 2.2 Laser damage testing

The laser system used for these tests was a Nd: glass zig-zag slab amplifier phase-conjugated laser system capable of producing a 25 J, 1053 nm wavelength, 14 ns FWHM pulses of near diffraction-limited beam quality, single shot to 2 Hz. All fluence values, as measured with a calibrated scientific grade camera at the plane of the sample, are reported normal to the propagation direction. Typical contrast as imaged on the sample was ~26% in the central 70% of the approximately 6 x 6 mm<sup>2</sup> square beam. The actual beam area on the substrate was ~0.5 cm<sup>2</sup> due to the 45° angle of incidence. The peak fluence within the beam was typically two times the average fluence. The repetition rate of the laser used during these tests was 0.3 Hz. An additional camera was used with the reflected light to image the surface and obtain the location of the particles in the beam. An online, long-working-distance microscope was the 3<sup>rd</sup> camera used during laser irradiation. It had sufficient resolution to observe the plasma generated during a laser shot. For the experiments reported here, the 3<sup>rd</sup> camera was primarily used to identify possible damage during the conditioning shots prior to Ti particle application. A similar setup of the laser system is described in detail in [11].

Prior to contaminant-induced laser damage testing, the surface of each sample of capping layer materials was first laser conditioned by ramping the fluence from 1 J/cm<sup>2</sup> to 15 J/cm<sup>2</sup> in steps of 0.2 J/cm<sup>2</sup> (1053 nm, 14 ns). Laser conditioned surfaces were then contaminated with evenly distributed Ti particles of either spherical shape or irregular-shaped filings,

which were sprinkled onto the test area by tapping a sheet of paper containing a layer of the particles approximately 30 cm above the sample. The Ti spheres were purchased commercially (Goodfellow, USA) and the filings were home-made by filing a high purity Ti plate. The fabricated filings were then separated by size using particle sieves in 100 micron increments. The spheres had a nominal  $30 \pm 16 \mu\text{m}$  in diameter, and the filings had an average length of  $250 \mu\text{m}$  and a width of  $40\text{-}50 \mu\text{m}$ . Each sample was placed vertically in the testing system with a beam incident angle of  $45^\circ$ .

For the damage initiation study, the surfaces, with the deposited Ti particles, were exposed to a single shot of the laser pulse (p-polarized, 1053 nm, 14 ns) at an average fluence of  $10 \text{ J/cm}^2$ . For damage growth investigation, the initiated damage sites at the locations of a Ti particle were exposed to sequential shots with a given laser fluence. Laser exposure was let out in sets of 50 shots at 0.3 Hz. The sample surface under laser irradiation was monitored in real time by an online microscope camera. Laser exposure was halted when damage grew rapidly over the entire testing area or when two nearby sites began merging together.

### **2.3 Optical Microscopy**

Laser-exposed samples were characterized by a high resolution scanning optical microscope ( $\sim 0.9 \mu\text{m}/\text{pixel}$ , Benchmark, View MicroMetrology) for particle distribution, damage morphology and topology, respectively. Analysis of images from both online (with resolution  $\sim 12$  microns per pixel) and offline microscopes also led to the assessment of the evolution of the damage size in terms of the number of laser shots and to the calculation of damage growth coefficient of coatings with different capping layer composition due to the laser-Ti particle interaction.

## **3. Results and Discussion**

The typical morphologies of Ti particles used for the current study are shown in Figure 1. While the commercially available Ti particles are all smooth surface spheres (Figure 1a), the homemade filings exhibit irregular shapes with a relatively rough surfaces (Figure 1b). The sprinkled Ti spherical particles on the  $\text{Al}_2\text{O}_3$  capping layer surface are shown in Figure 2a. While variations in size are inevitable, the majority of the particles on the surface were approximately  $30 \mu\text{m}$  in diameter. The apparently larger particles were usually aggregates of smaller ones. Exposure to a single shot laser at  $45^\circ$  off normal with an average fluence of  $10 \text{ J/cm}^2$  leads to damage on the capping surface which is characterized by the distorted oval features (white color) in Figure 2b. A comparison of Figure 2a to Figure 2b shows that nearly all of the damage sites are at the locations of a Ti particle. However, some damage sites appear at locations where no Ti particles are found, indicating that some particles were relocated during transportation of the test sample between microscope imaging and laser damage testing. However, no original particles were observed after the laser shot. The size of these damage sites ranged from a few  $\mu\text{m}$  to approximately  $400 \mu\text{m}$  along the longer dimension. The damage sites had an approximate depth from the pristine layer ranging between  $250 \text{ nm}$  and  $350 \text{ nm}$  [17]. Since the capping layer was  $\sim 360 \text{ nm}$  thick, the result suggests that damage was caused by a partial to full removal of the capping materials at the damage sites.

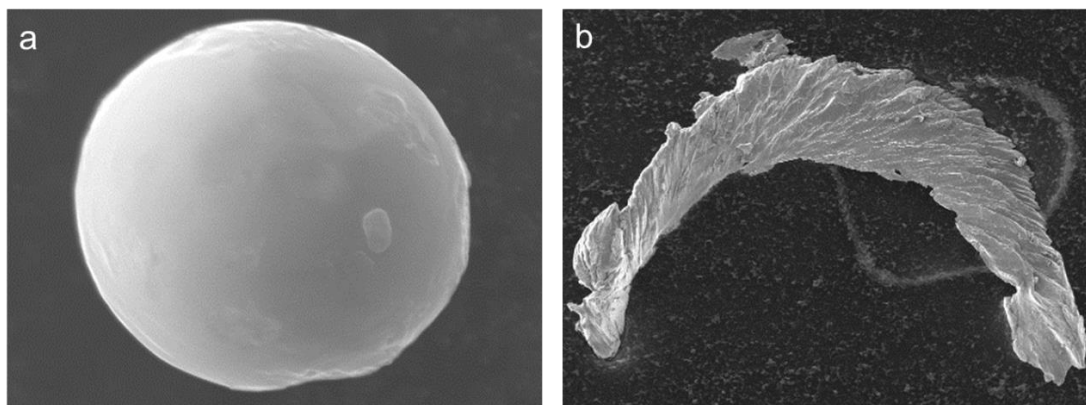


**Figure 1.** Representative morphology of Ti particles from (a) commercially available Ti spheres and (b) home-made Ti filings. The Ti sphere shown has an  $18 \mu\text{m}$  diameter. The length of the Ti filings shown is  $\sim 250 \mu\text{m}$ ; its width ranges between  $40\text{-}50 \mu\text{m}$ .

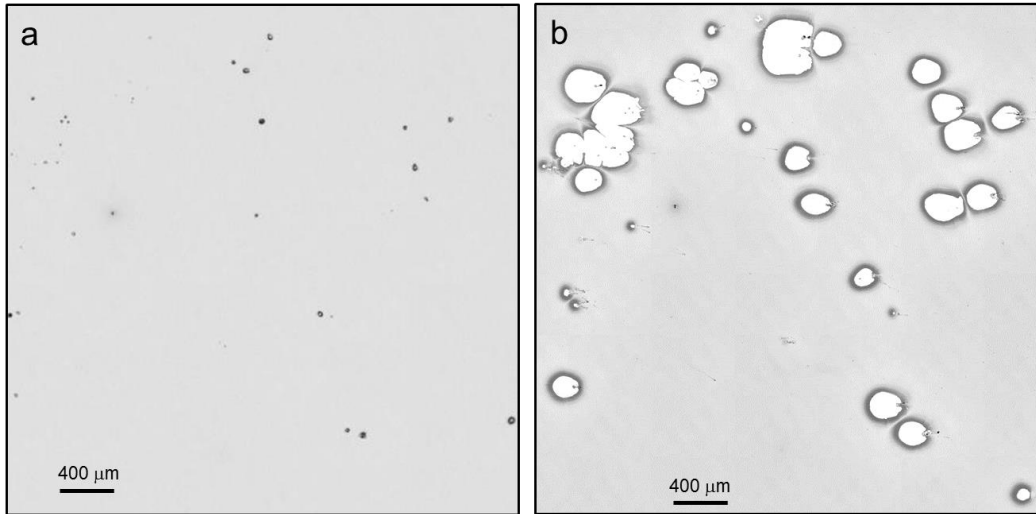


**Figure 2:** Optical images of the  $\text{Al}_2\text{O}_3$  capping layer surface: (a) with spherical Ti particle sprinkled on before laser shot and (b) after a single laser shot.

The distribution of Ti spheres on the  $\text{SiO}_2$  capping layer surface (Figure 3a) was similar to that on the  $\text{Al}_2\text{O}_3$  capping layer surface. The surface was also modified at the locations of a Ti particle after one laser shot of identical conditions. However, the change in the capping layer is drastically different from that on the  $\text{Al}_2\text{O}_3$  surface. There is no surface layer delamination. Instead the modified sites all show a depression or erosion from the original surface with the depth of approximately 150 nm [17]. On both capping layers, associated with the surface modification, there are trails of Ti droplets printing along the beam direction at the damage vicinity.

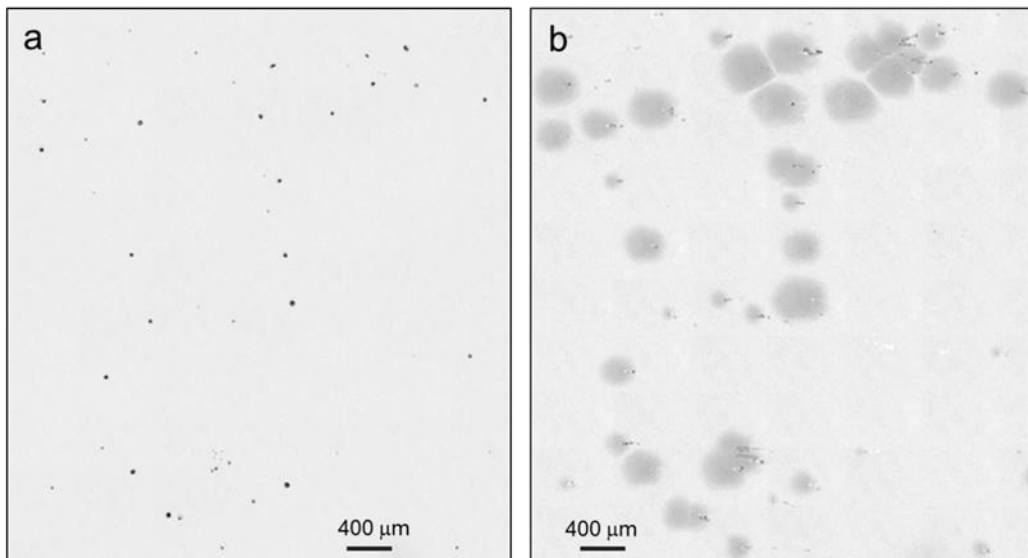


**Figure 3:** Optical images of the  $\text{SiO}_2$  capping layer surface: (a) with spherical Ti particle sprinkled on before laser shot and (b) after a single laser shot.

The response of the two capping layers to the laser-Ti filing interaction is opposite to that of the laser-Ti spherical particle interaction. With Ti filing particles, the interaction-induced damage is more pronounced on  $\text{SiO}_2$  than on  $\text{Al}_2\text{O}_3$ . Figure 4a shows the surface of the  $\text{Al}_2\text{O}_3$  capping layer after the laser exposure. At the Ti filing location, there is

essentially no surface modification except one. Instead, the surface contains fragmented Ti particles at the original Ti locations. The shape of the resulting fragments (the dark spots in the image) resembles the original croissant shape of the Ti filings. Figure 4b shows the surface of the SiO<sub>2</sub> capping layer after the laser exposure. Near the original particle location, fragmented Ti particles are observed. Along the beam propagation direction, the surface at the location where the fragmented particle resides is fractured. The side towards the beam direction, on the other hand, shows optical features similar to those observed in Figure 3b, which may result from a similar surface depression.

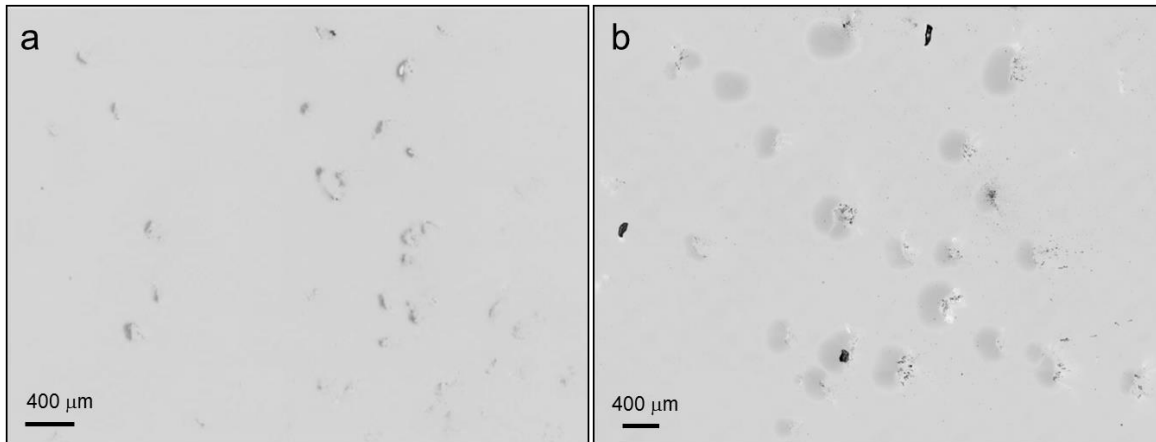


**Figure 4:** Optical images of the capping layer surface after one laser shot at the presence of irregularly shaped Ti filings: (a) Al<sub>2</sub>O<sub>3</sub> surface and (b) SiO<sub>2</sub> surface.

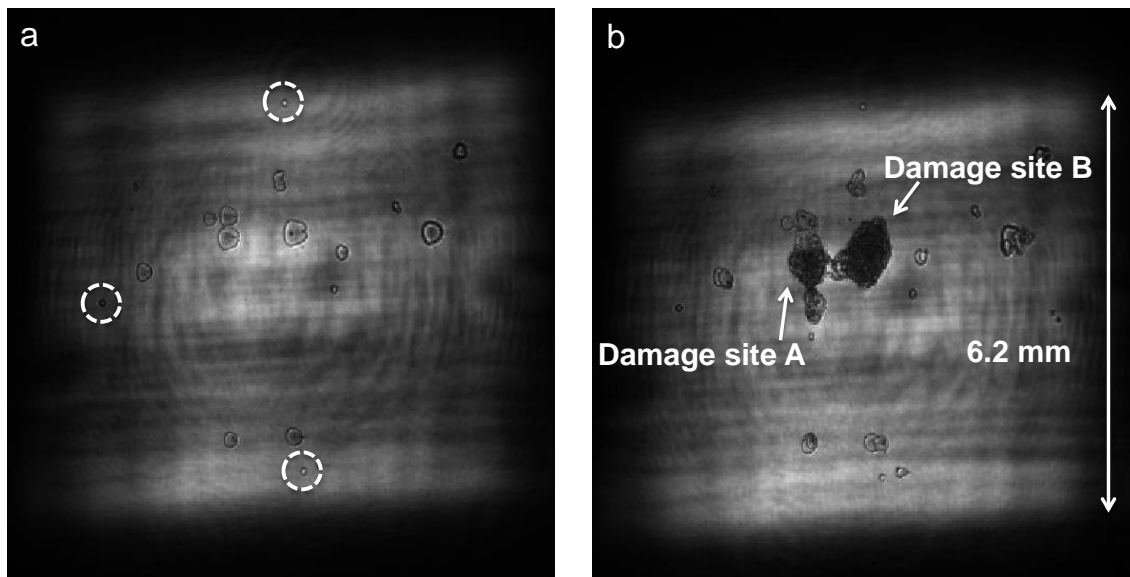


**Figure 5:** Reflected camera images of the Al<sub>2</sub>O<sub>3</sub> capping layer surface pre (a) and post 50 shots (b) at beam average fluence of 10 J/cm<sup>2</sup>.

Figure 5 shows reflected camera images of pre- and post- 50 shots at an average fluence of 10 J/cm<sup>2</sup> on the Al<sub>2</sub>O<sub>3</sub> capped surface after an initiation fluence of 10 J/cm<sup>2</sup> at the locations of the spherical Ti particles. The dotted circles in Figure 5a are fiducials used to register local fluence of the damage sites. Several initiated damage sites are seen in the initial image. After 50 shots, several sites are seen to grow. The two sites that we monitored for understanding the growth are indicated in the figure by the two arrows (site A and B). The reason that the exposure was curtailed at 50 shots is that the

two damages sites were starting to merge. The two apparent growing sites show directional growth, with the vertical direction being the fast-growing route.

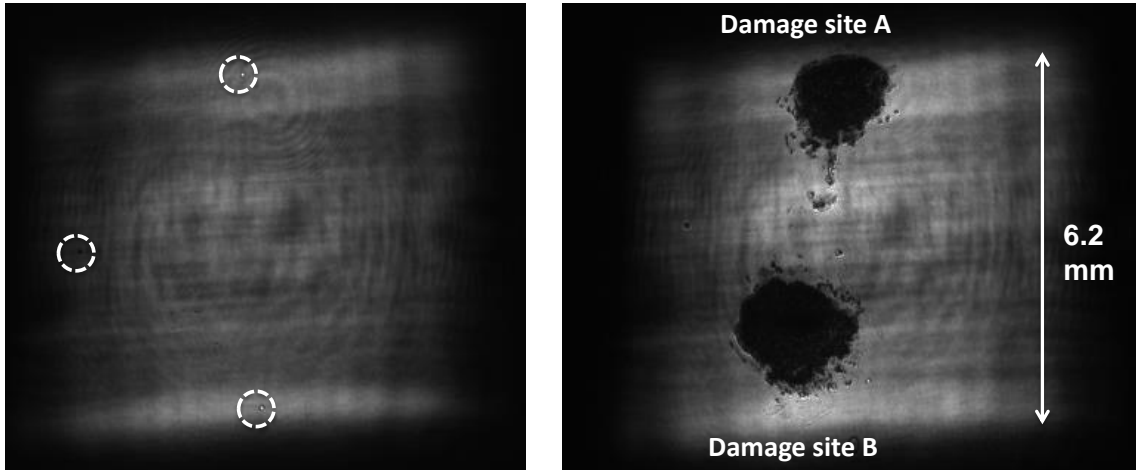


**Figure 6:** Reflected camera images of the SiO<sub>2</sub> capping layer surface pre (a) and post 138 shots (a) at beam average fluence of 25 J/cm<sup>2</sup>.

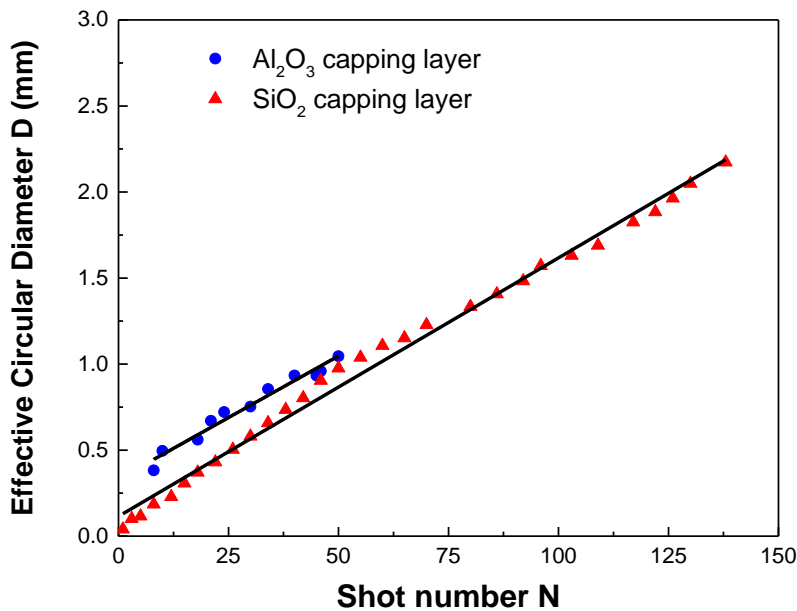


Figure 7: The dependence of the effective circular diameter of the growing sites on the number of the sequential laser exposure on the two different capping layers.

Figure 6 shows the reflected camera images of pre and post 138 shots at an average fluence of 25 J/cm<sup>2</sup> on the SiO<sub>2</sub> capped surface after an initiation of 10 J/cm<sup>2</sup> at the locations of the spherical Ti particles. Although no initiated sites are visible in the pre-shot image, it was confirmed by offline microscopic analysis that there were several initiated sites in the investigated region. Laser exposure was stopped at 138 shots as the two growing sites began to merge with other adjacent small sites. The dotted circles in Figure 6a are fiducials used to register the local fluence of the damage sites. After ~50 shots, several sites are seen to grow. The two sites that we monitored for understanding the damage growth are

indicated in the figure by the two arrows (site A and B). Similar directional growth modes are also observed in the two apparent growing sites, which show that the vertical direction is the preferred growing direction.

The average effective circular diameter of the two growing sites is displayed in Figure 7. For both capping layer materials, the damage growth or the rate of change of the effective diameter of the damage sites exhibits similar and nearly linear dependence on the number of laser shots; although the capping layers are made of different materials and post-initiation fluence exposures are different. The data are fitted by a straight line using least squares and the slope of the fitted straight line is summarized in Table 1.

Table 1: Summary of the damage growth coefficient on two different type of capping layers

Capping Material	Exposure Fluence	dD/dN (mm/per shot)
Al <sub>2</sub> O <sub>3</sub>	10	1.43 x 10 <sup>-2</sup>
SiO <sub>2</sub>	25	1.50 x 10 <sup>-2</sup>

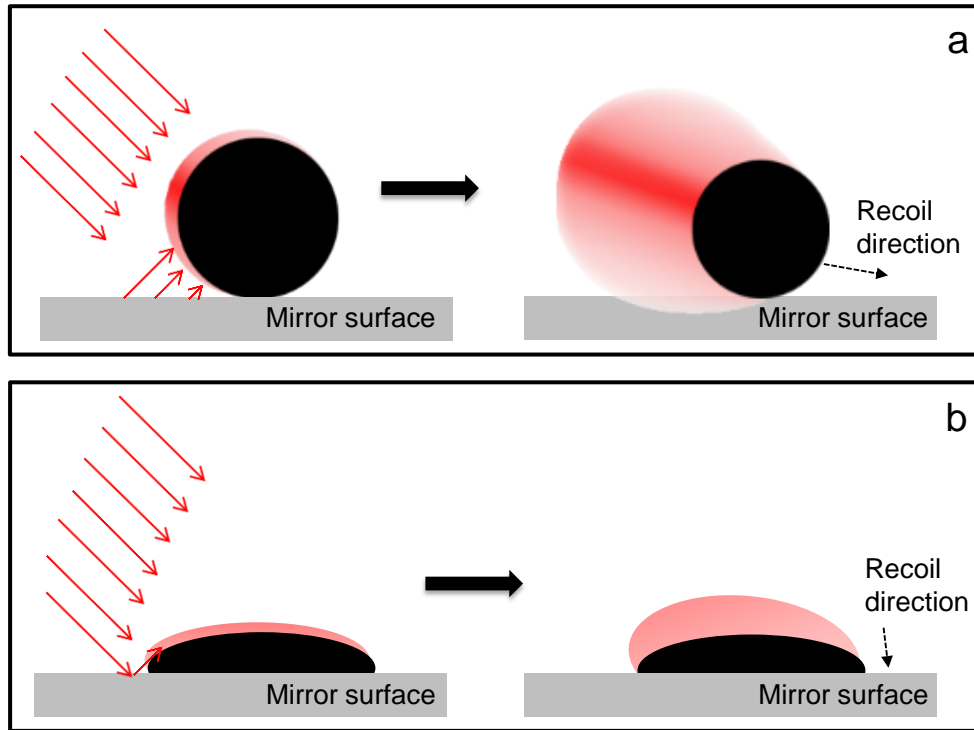


**Figure 8.** Schematics showing the laser induced plasma formation and particle recoil on reflective surface with (a) a spherical Ti particle, and (b) an irregularly shaped Ti particle.

Laser light impinging on a metal can elevate its surface temperature. If the fluence is sufficiently high, the surface temperature can rise beyond the vaporization temperature. Subsequent interaction between the laser and vapor can cause further temperature elevation and result in plasma formation. Depending upon the beam direction and the shape of the metal particle, the thermally-active plasma plume may or may not intercept the surface on which the metallic particle resides. In our earlier estimate [17], the fluence threshold for plasma formation was about 4.4 J/cm<sup>2</sup> for a 14 ns pulse. Thus under the present irradiation of 10 J/cm<sup>2</sup>, plasma formation is expected. Besides transporting thermal energy, the formation of the plasma at the Ti particle surface can also lead to the recoil of the fragmented droplets and the remaining

particle itself. The recoil momentum depends on the ejection direction of the plasma, which is strongly correlated to the shape of the particle.

For a spherical particle, the combination of oblique incidence and reflective surfaces between the sphere and the substrate leads to an increased absorption on the Ti surface. An analysis of this process has been given in Ref. [17], showing that the maximum laser absorption occurs at an angle of  $80^\circ$  from the surface normal (on the side toward the incoming beam). Consequently, plasma is produced; expanding toward the beam incidence direction and intersecting the capping layer (Figure 8a). In turn, the hot remnants are expelled in the opposite direction along the capping layer surface. Each of these processes can lead to surface modification or damage, depending on the thermal-mechanical robustness of the capping materials. Because the thermal expansion coefficient of  $\text{Al}_2\text{O}_3$  is 15 times larger than that of  $\text{SiO}_2$ , the thermal-induced mechanical stress on the  $\text{Al}_2\text{O}_3$  capping layer is significantly larger than that experienced by the  $\text{SiO}_2$ . The mechanical stress differential between the  $\text{Al}_2\text{O}_3$  capping layer and the layer below can lead to the observed delamination. This mechanism is illustrated in Figure 8a.

For the irregularly shaped Ti particle, under similar laser fluence, plasma formation is again expected. However, because the Ti filing particles lie mostly flat on the surface, multiple reflections between the substrate surface and the surface of the metal particle are greatly diminished (Figure 8b). Thus we do not expect an increased absorption like that observed in the spherical particle. Consequently, the surface plasma will primarily be along the beam incidence direction of  $45^\circ$ . The overlap between the plasma and the capping surface is expected to be small. Similarly, the ejection of the plasma plume will result in the recoil of the remnants mostly along the beam propagation direction. Since the recoil angle is around  $45^\circ$ , the vertical component of the recoil momentum will be over 4 times larger than that with the spherical particle, potentially delivering a large mechanical impact on the capping surface. Because the mechanical toughness of  $\text{Al}_2\text{O}_3$  is 10 times larger than that of  $\text{SiO}_2$ , we hypothesize that this disparity is responsible for the observed difference in response to laser-induced damage. Furthermore, the strong mechanical toughness along with the large vertical recoil momentum is responsible for the fragmentation of the Ti filing on the  $\text{Al}_2\text{O}_3$  capping layer. This mechanism is depicted in Figure 8b.

#### 4. Conclusion

In summary, laser damage testing at oblique incidence shows that the laser-contaminant interaction on HR multilayer coatings leads to modification or damage to the surface protective capping layer. The damage behavior is strongly dependent on the shape of contaminant particles and composition of the capping material. For laser interaction with a spherical Ti particle, the damage is related to the thermal properties of the capping materials. For laser interaction with irregularly-shaped particles, the damage is related to the mechanical property of the capping material. Specifically, in the presence of the spherical Ti contaminant, the  $\text{Al}_2\text{O}_3$  capping layer shows much more severe damage than that of  $\text{SiO}_2$ , because  $\text{Al}_2\text{O}_3$  has a thermal expansion coefficient that is 15 times larger than that of the  $\text{SiO}_2$ . On the other hand, in the presence of the Ti filings, the damage on the  $\text{SiO}_2$  capping layer is more pronounced as the mechanical toughness of  $\text{Al}_2\text{O}_3$  is 10 times larger than that of  $\text{SiO}_2$ . In terms of the growth of the initiated sites, preliminary results show that damage size grows linearly with the number of exposing laser shots. Overall, our results suggest that a material with a strong mechanical toughness, but a small thermal expansion coefficient, may be effective for use as a capping material to protect against debris-induced laser ablation and damage on  $1\omega$  high power dielectric coating mirrors.

#### Acknowledgements

This work was performed under the auspices of the U.S. Department of Energy by Lawrence Livermore National Laboratory under Contract DE-AC52-07NA27344 and funded through Laboratory Directed Research and Development Grant 14-ERD-098. We would like to thank Gabe Guss, John Adams, and Raluca Negres for making fiducials, William G. Hollingsworth for performing the laser damage testing and optical microscope imaging, and Chantel Aracne-Ruddle for Ti filings separation. [LLNL-CONF-680222]

#### References

- [1] Stolz, C. J., "Status of NIF mirror technologies for completion of the NIF facility," Proc. of SPIE. 7107, 710115 (2008).
- [2] Pinot, B., Leplan, H., Houbre, F. *et al.*, "Laser megajoule 1.06- $\mu\text{m}$  mirror production with very high laser damage threshold," Proc. of SPIE. 4679, 234-241 (2002).

- [3] Oliver, J. B., Rigatti, A. L., Howe, J. D. *et al.*, "Thin-film polarizers for the OMEGA EP laser system," Proc. SPIE. 5991, 599119-1-8 (2005).
- [4] Jitsuno, T., Murakami, H., Kato, K. *et al.*, "Recent progresses on insights of laser damage mechanisms and influence of contamination in optics," Proc. of SPIE. 8786, 87860B-6 (2013).
- [5] Gourdin, W. H., Dzenitis, E. G., Martin, D. A. *et al.*, "Insitu surface debris inspection and removal system for upward-facing transport mirrors of the National Ignition Facility," Proc. of SPIE. 5647, 107-119 (2005).
- [6] Ling, X. L., Wang, G., Zhao, Y. N. *et al.*, "Laser-induced damage of the optical coatings due to organic contamination in vacuum," Appl. Surf. Sci., 270, 346-351 (2013).
- [7] Carniglia, C. K., Apfel, J. H., Allen, T. H. *et al.*, "Recent damage results on silica/titania reflectors at 1 micron," NBS Special Pub., 568, 377 (1979).
- [8] Walton, C. C., Genin, F. Y., Chow, R. *et al.*, "Effect of silica overlayers on laser damage of HfO<sub>2</sub>-SiO<sub>2</sub> 56 degrees incidence high reflectors," Proc. of SPIE. 2714, 550-559 (1996).
- [9] Wu, Z., Fan, Z., and Wang, Z., "Damage Threshold Dependence on Film Thickness," NIST Special Pub., 775, 321 (1988).
- [10] Bajt, S., Edwards, N. V., and Madey, T. E., "Properties of ultrathin films appropriate for optics capping layers exposed to high energy photon irradiation," Surf. Sci. Rep., 63(2), 73-99 (2008).
- [11] Norton, M. A., Stolz, C. J., Donohue, E. E. *et al.*, "Impact of contaminants on the laser damage threshold of 1 $\omega$  HR coatings," Proc. of SPIE. 5991, 5991001-9 (2005).
- [12] Stolz, C. J., Thomas, M. D., and Griffin, A. J., "BDS thin film damage competition," Proc. of SPIE. 7132, 71320C1-C7 (2008).
- [13] Oliver, J. B., Kupinski, P., Rigatti, A. L. *et al.*, "Stress compensation in hafnia/silica optical coatings by inclusion of alumina layers," Opt. Express, 20(15), 16596-16610 (2012).
- [14] Zhu, M., Yi, K., Li, D. *et al.*, "Study on the laser-induced damage performance of HfO<sub>2</sub>, Sc<sub>2</sub>O<sub>3</sub>, Y<sub>2</sub>O<sub>3</sub>, Al<sub>2</sub>O<sub>3</sub> and SiO<sub>2</sub> monolayer coatings," Proc. of SPIE. 8885, 8885081-8 (2013).
- [15] Henyk, M., Wolfframm, D., and Reif, J., "Ultra short laser pulse induced charged particle emission from wide bandgap crystals," Appl. Surf. Sci., 168(1-4), 263-266 (2000).
- [16] Reichling, M., Bodemann, A., and Kaiser, N., "Defect induced laser damage in oxide multilayer coatings for 248 nm," Thin Solid Films, 320(2), 264-279 (1998).
- [17] Qiu, S. R., Norton, M. A., Raman, R. N. *et al.*, "Impact of laser-contaminant interaction on the performance of the protective capping layer of 1 omega high-reflection mirror coatings," Appl. Opt., 54(29), 8607-8616 (2015).
- [18] Oliver, J. B., Howe, J., Rigatti, A. *et al.*, "High precision coating technology for large aperture NIF optics," Optical Interference Coatings, OSA Technical Digest (Optical Society of America, Washington, DC, ThD2 (2001).
- [19] Anzellotti, J. F., Smith, D. J., Sczupak, R. J. *et al.*, "Stress and environmental shift characteristics of HfO<sub>2</sub>/SiO<sub>2</sub> multilayer coatings," Proc. of SPIE. 2966, 258-264 (1996).